

LA-UR-15-20091 (Accepted Manuscript)

A Long-Lived Relativistic Electron Storage Ring Embedded in Earth's Outer Van Allen Belt

Baker, D. N.
Henderson, Michael Gerard
Friedel, Reinhard Hans Walter
Reeves, Geoffrey D.

Provided by the author(s) and the Los Alamos National Laboratory (2016-03-29).

To be published in: Science

DOI to publisher's version: 10.1126/science.1233518

Permalink to record: <http://permalink.lanl.gov/object/view?what=info:lanl-repo/lareport/LA-UR-15-20091>

Disclaimer:

Approved for public release. Los Alamos National Laboratory, an affirmative action/equal opportunity employer, is operated by the Los Alamos National Security, LLC for the National Nuclear Security Administration of the U.S. Department of Energy under contract DE-AC52-06NA25396. Los Alamos National Laboratory strongly supports academic freedom and a researcher's right to publish; as an institution, however, the Laboratory does not endorse the viewpoint of a publication or guarantee its technical correctness.

A Long-Lived Relativistic Electron Storage Ring Embedded in Earth's Outer Van Allen Belt

D. N. Baker,^{1*} S. G. Kanekal,² V. C. Hoxie,¹ M. G. Henderson,³ X. Li,¹ H. E. Spence,⁴ S. R. Elkington,¹ R. H. W. Friedel,³ J. Goldstein,⁵ M. K. Hudson,⁶ G. D. Reeves,³ R. M. Thorne,⁷ C. A. Kletzing,⁸ S. G. Claudepierre⁹

¹Laboratory for Atmospheric and Space Physics, University of Colorado, Boulder, CO, USA. ²Goddard Space Flight Center, Greenbelt, MD, USA. ³Los Alamos National Laboratory, Los Alamos, NM, USA.

⁴Institute for the Study of Earth, Oceans, and Space, University of New Hampshire, Durham, NH, USA.

⁵Space Science and Engineering Division, Southwest Research Institute, San Antonio, TX, USA.

⁶Department of Physics and Astronomy, Dartmouth College, Hanover, NH, USA. ⁷Department of Atmospheric and Oceanic Sciences, University of California – Los Angeles, Los Angeles, CA, USA.

⁸Department of Physics and Astronomy, University of Iowa, Iowa City, IA, USA. ⁹The Aerospace Corporation, Los Angeles, CA, USA.

*To whom correspondence should be addressed. E-mail: daniel.baker@lasp.colorado.edu

Since their discovery over 50 years ago, the Earth's Van Allen radiation belts have been considered to consist of two distinct zones of trapped, highly energetic charged particles. The outer zone is comprised predominantly of mega-electron volt (MeV) electrons that wax and wane in intensity on time scales ranging from hours to days depending primarily on external forcing by the solar wind. The spatially separated inner zone is comprised of commingled high-energy electrons and very energetic positive ions (mostly protons), the latter being stable in intensity levels over years to decades. In situ energy-specific and temporally resolved spacecraft observations reveal an isolated third ring, or torus, of high-energy ($E > 2$ MeV) electrons that formed on 2 September 2012 and persisted largely unchanged in the geocentric radial range of 3.0 to ~3.5 Earth radii for over four weeks before being disrupted (and virtually annihilated) by a powerful interplanetary shock wave passage.

The magnetically confined radiation zones surrounding the Earth were the first major discovery of the Space Age in 1958 (1–4). Long-term observations of these energetic particle populations subsequently have shown dramatic, highly dynamic changes of the outer Van Allen belt. Previous, rather sparse measurements of the radiation environment suggested that powerful acceleration events for relativistic electrons occur on time scales ranging from minutes (5, 6) to many hours (7, 8). Thus, there has been direct as well as circumstantial evidence that an immensely powerful and efficient accelerator operates within the terrestrial magnetosphere just a few thousand kilometers above the Earth's surface.

On 30 August 2012, twin NASA spacecraft, the Radiation Belt Storm Probes (RBSP), were launched into highly elliptical, low-inclination orbits around the Earth. The RBSP satellites are fully instrumented with identical energetic particle, plasma, magnetic field, and plasma wave sensors to measure and thoroughly characterize the radiation belt regions (9). The scientific payloads on board the RBSP spacecraft (renamed the Van Allen Probes mission by NASA at a formal ceremony on 9 November 2012) have unprecedented detection sensitivity, energy resolution, and temporal sampling capability. In particular, the Relativistic Electron-Proton Telescope (REPT) experiment (10) measures the key ~1 MeV to ~20 MeV electron population throughout the RBSP orbit which extends from geocentric distances of $r = 1.2 R_E$ to $r = 5.8 R_E$ ($1R_E$, Earth radius – 6372 km). The REPT sensors were among the first instruments turned on (1 September 2012) and have been returning nearly continuous data since that time from both Van Allen Probes spacecraft.

Prior key measurements of Earth's radiation environment have been made (11–13), but some of the longest and most comprehensive radiation belt observations previously have come from sensors on board the Solar, Anomalous, and Magnetospheric Particle Explorer (SAMPEX) mission (14). This spacecraft made low-Earth orbit (LEO) observations of inner and outer zone particles from its launch in July 1992 until its recent atmospheric reentry and demise on 13 November 2012 (15, 16). SAMPEX measured $E > 1$ MeV electrons at the near-Earth foot of magnetic field lines but never was able to look into the “throat” of the radiation belt accelerator in the magnetospheric equatorial plane. This contrasts dramatically with the REPT-A and REPT-B instrument data collected by the Van Allen Probes from 1 September 2012 through early October 2012 (Fig. 1). These data show that a powerful electron acceleration event was already in progress as the instruments were first turned on. The entire outer radiation belt was enhanced in electron flux from $E \sim 2.0$ MeV (Fig. 1A) up to energies well above the $6.2 < E < 7.5$ MeV channel (Fig. 1C). At this time, the radiation belt populations clearly had the expected double-belt structure with an inner zone, an outer zone, and a “slot” region of greatly diminished intensity separating the two.

What is most striking (and unexpected) is the clear emergence of a separate, previously unseen belt, or “storage ring,” of high-energy electrons that stands out clearly after 2 September. This belt is evident in the $E = 4.0$ – 5.0 MeV range (Fig. 1B) and is the dominant flux feature in the $E = 5.0$ – 6.2 MeV energy range (Fig. 1C). This distinctive ring of highly relativistic electrons persists, changing only gradually, until its abrupt and almost complete disappearance late on 1 October. While the inner zone, the slot region, and the relativistic storage ring ($3.0 < L^* < \sim 3.5$) change relatively little over this four-week period, the more distant part of the outer Van Allen belt shows huge dynamical changes with new electron populations appearing at $L^* > 4.0$ beginning on about 7 September and intensifying greatly over a period of two weeks. Subsequently, the outermost parts of the outer Van Allen zone grew and diminished further with little effect on the storage ring feature until the abrupt demise of virtually the entire outer zone electron population at the end of 1 October. Other electron sensor systems on board the Van Allen Probes spacecraft, overlapping partially in energy coverage with the REPT sensors, also detected the storage ring feature (17).

The distinct storage ring feature is more clearly evident in the meridional plane projection of 4.0–5.0 MeV electrons from the combined REPT-A and REPT-B instrument records (Fig. 2). In the earliest observational phase (1–3 September) the expected two-belt structure of the Van Allen zones is clear (Fig. 2A). In the next phase from 3 to 6 September, the relativistic storage ring was formed (Fig. 2B) probably largely by erosion and loss of the more distant parts of the outer zone. It then persisted in a remarkably stable fashion (Fig. 2, C and D) throughout the

remainder of September until its almost complete annihilation early in October 2012.

We note that powerful “injection” of high-energy electrons and protons deep into the inner part of the Earth’s magnetosphere on 24 March 1991 (5, 18, 19) was observed by instruments on board the CRRES spacecraft (13). It was a highly impulsive event caused by an exceptionally strong interplanetary shock wave (5, 6). This March 1991 event was a stark example of the sudden appearance of a newly energized population of both protons and electrons in a localized portion of the slot region of the radiation belts that normally is nearly devoid of very energetic particles (19, 20). This prior event contrasts with the storage ring feature observed by the Van Allen Probes sensors: The storage ring clearly resulted largely from loss of the more distant portion of the outer zone electron population rather than fresh, localized injection of the March 1991 type. The original acceleration of the electron population (prior to the turn-on of REPT on 1 September) that eventually formed the storage ring may have resulted either from local wave heating (21, 22) or from enhanced radial diffusion (23, 24) or both.

Based on prior radiation belt research [e.g., (7, 15)], the outer Van Allen zone electron populations would be expected to respond rather directly to changes in the solar wind, interplanetary magnetic field (IMF), and geomagnetic activity. Indeed, the development of the storage ring feature itself (Fig. 3) was closely associated with loss of outer belt electrons following passage of an interplanetary shock wave on 3 September, seen as a sharp increase in solar wind speed (Fig. 3B) and abrupt change in the IMF (Fig. 3C). Subsequently, a new population of highly relativistic electrons emerged at a region around $L^* \sim 4.0$ and grew in intensity and spatial extent (Fig. 3A) following a high-speed solar wind episode (Fig. 3B) on 5 September. Another such period of high-energy electron flux diminution, reappearance, and intensification was seen from ~21 September through to 1 October (Fig. 3A), again this sequence occurring in the wake of a powerful high-speed solar wind stream on 20–21 September (Fig. 3B). As noted above, one of the most abrupt and striking features of the entire data set was the nearly complete disappearance of the entire outer zone electron population late on 1 October associated with another interplanetary shock wave (Fig. 3, B and C) and relatively strong geomagnetic storm (seen in Dst, which measures global magnetic field disturbance, Fig. 3D).

Figure 3A shows that for the period of 1–4 September, the average plasmopause boundary was relatively close to the Earth ($L^* \sim 3$) and a powerful outer zone electron acceleration event was occurring in the low plasma-density region outside the plasmasphere. However, from ~4 September until ~6 October, the plasmopause was much farther outward, ranging at $L^* > 4$. Thus, the storage ring feature as well as most of the outer Van Allen zone $E > 4.5$ MeV electron population was inside the high-density plasmasphere. However, in the traditional picture the outer zone electron belt would largely be outside the plasmasphere and the slot region inside the plasmasphere outer boundary (21–23, 25).

The radiation belt particle populations are determined by a complex superposition of acceleration, transport, and loss processes modulated by their interactions with plasma waves (24). We are now seeing unexpected radiation belt structures (Fig. 4), but have yet to fully understand them in the context of present radiation belt theory.

References and Notes

1. J. A. Van Allen *et al.*, *Jet Propuls.* **28**, 588 (1958).
2. J. A. Van Allen, The geomagnetically trapped corpuscular radiation. *J. Geophys. Res.* **64**, 1683 (1959). doi:10.1029/JZ064i011p01683
3. J. A. Van Allen, L. A. Frank, Radiation around the Earth to a radial distance of 107,400 km. *Nature* **183**, 430 (1959). doi:10.1038/183430a0
4. S. C. Freden, R. S. White, Protons in the Earth’s magnetic field. *Phys. Rev. Lett.* **3**, 9 (1959). doi:10.1103/PhysRevLett.3.9
5. J. B. Blake, W. A. Kolasinski, R. W. Fillius, E. G. Mullen, Injection of electrons and protons with energies of tens of MeV into $L < 3$ on 24 March

1991. *Geophys. Res. Lett.* **19**, 821 (1992). doi:10.1029/92GL00624
6. X. Li *et al.*, Simulation of the prompt energization and transport of radiation belt particles during the March 24, 1991 SSC. *Geophys. Res. Lett.* **20**, 2423 (1993). doi:10.1029/93GL02701
7. D. N. Baker *et al.*, Relativistic electron acceleration and decay time scales in the inner and outer radiation belts: SAMPEX. *Geophys. Res. Lett.* **21**, 409 (1994). doi:10.1029/93GL03532
8. R. B. Horne *et al.*, Timescale for radiation belt electron acceleration by whistler mode chorus waves. *J. Geophys. Res.* **110**, A03225 (2005). doi:10.1029/2004JA010811
9. B. H. Mauk *et al.*, Science objectives and rationale for the Radiation Belt Storm Probes mission. *Space Sci. Rev.* 10.1007/s11214-012-9908-y (2012).
10. D. N. Baker *et al.*, The Relativistic Electron-Proton Telescope (REPT) instrument on board the Radiation Belt Storm Probes (RBSP) spacecraft: Characterization of Earth’s radiation belt high-energy particle populations. *Space Sci. Rev.* 10.1007/s11214-012-9950-9 (2012).
11. Since the initial Van Allen belt discovery, there have been many missions that have measured key aspects of the radiation properties around the Earth. Some of these have been from “operational” satellite systems such as the National Oceanic and Atmospheric Administration (NOAA) weather satellites in geostationary Earth orbit (GEO) (www.oso.noaa.gov/goesstatus) or polar low-Earth (LEO) (www.oso.noaa.gov/poesstatus) orbits. Other measurements have been made using sensors on board operational GEO spacecraft or the Global Positioning Satellite (GPS) timing and navigation constellation of spacecraft as well as the Polar and Cluster scientific satellites (12). These prior satellites have provided key long-term monitoring of radiation belt changes, but have generally not made measurements directly in the heart of the radiation belt regions. Only the Combined Release and Radiation Effects Satellite (CRRES) mission (13) operated briefly (1990–91) in the heart of the radiation belts but lacked the background rejection and the temporal, energy, and spatial resolution now provided by the dual Van Allen Probes.
12. R. H. W. Friedel, G. D. Reeves, T. Obara, Relativistic electron dynamics in the inner magnetosphere — a review. *J. Atmos. Sol. Terr. Phys.* **64**, 265 (2002). doi:10.1016/S1364-6826(01)00088-8
13. M. H. Johnson, J. Kierein, Combined Release and Radiation Effects Satellite (CRRES): Spacecraft and mission. *J. Spacecr. Rockets* **29**, 556 (1992). doi:10.2514/3.55641
14. D. N. Baker *et al.*, An overview of the Solar Anomalous, and Magnetospheric Particle Explorer (SAMPEX) mission. *IEEE Trans. Geosci. Rem. Sens.* **31**, 531 (1993). doi:10.1109/36.225519
15. X. Li, M. Temerin, D. N. Baker, G. D. Reeves, Behavior of MeV electrons at geosynchronous orbit during last two solar cycles. *J. Geophys. Res.* **116**, A11207 (2011). doi:10.1029/2011JA016934
16. D. N. Baker, J. E. Mazur, G. M. Mason, SAMPEX to reenter atmosphere: Twenty-year mission will end. *Space Weather* **10**, S05006 (2012). doi:10.1029/2012SW000804
17. See data and methods in the accompanying supplementary materials on Science Online.
18. A. L. Vampola, A. Korth, electron drift echoes in the inner magnetosphere. *Geophys. Res. Lett.* **19**, 625 (1992). doi:10.1029/92GL00121
19. E. G. Mullen, M. S. Gussenhoven, K. Ray, M. Violet, A double-peaked inner radiation belt: cause and effect as seen on CRRES. *IEEE Trans. Nucl. Sci.* **38**, 1713 (1991). doi:10.1109/23.124167
20. D. H. Brautigam, *JASTP* **64**, 1709 (2002).
21. R. B. Horne *et al.*, Wave acceleration of electrons in the Van Allen radiation belts. *Nature* **437**, 227 (2005). doi:10.1038/nature03939 Medline
22. Y. Y. Shprits *et al.*, Acceleration mechanism responsible for the formation of the new radiation belt during the 2003 Halloween solar storm. *Geophys. Res. Lett.* **33**, L05104 (2006). doi:10.1029/2005GL024256
23. X. Li, D. N. Baker, T. P. O’Brien, L. Xie, Q. G. Zong, Correlation between the inner edge of outer radiation belt electrons and the innermost plasmopause location. *Geophys. Res. Lett.* **33**, L14107 (2006). doi:10.1029/2006GL026294
24. R. M. Thorne, Radiation belt dynamics: The importance of wave-particle interactions. *Geophys. Res. Lett.* **37**, L22107 (2010). doi:10.1029/2010GL044990
25. L. R. Lyons, R. M. Thorne, Equilibrium structure of radiation belt electrons. *J. Geophys. Res.* **78**, 2142 (1973). doi:10.1029/JA078i013p02142
26. J. Goldstein, Plasmasphere response: Tutorial and review of recent imaging results. *Space Sci. Rev.* **124**, 203 (2006).

27. J. Goldstein, B. R. Sandel, W. T. Forrester, M. F. Thomsen, M. R. Hairston, Global plasmasphere evolution 22–23 April 2001. *J. Geophys. Res.* **110**, A12218 (2005). doi:10.1029/2005JA011282
28. R. E. Denton *et al.*, Magnetospheric electron density long-term (>1 day) refilling rates inferred from passive radio emissions measured by IMAGE RPI during geomagnetically quiet times. *J. Geophys. Res.* **117**, A03221 (2012). doi:10.1029/2011JA017274

Acknowledgments: This work was supported by RBSP-ECT funding provided by JHU/APL contract no. 967399 while EMFISIS work was supported on JHU/APL contract no. 921649 both under NASA's Prime contract no. NAS5-01072. All Van Allen Probes observations used in this study, along with display and analysis software, are publicly available at the Web site www.rbsp-ect.lanl.gov.

Supplementary Materials

www.sciencemag.org/cgi/content/full/science.1233518/DC1

Supplementary Text

Figs. S1 and S2

References

3 December 2012; accepted 5 February 2013

Published online 28 February 2013

10.1126/science.1233518

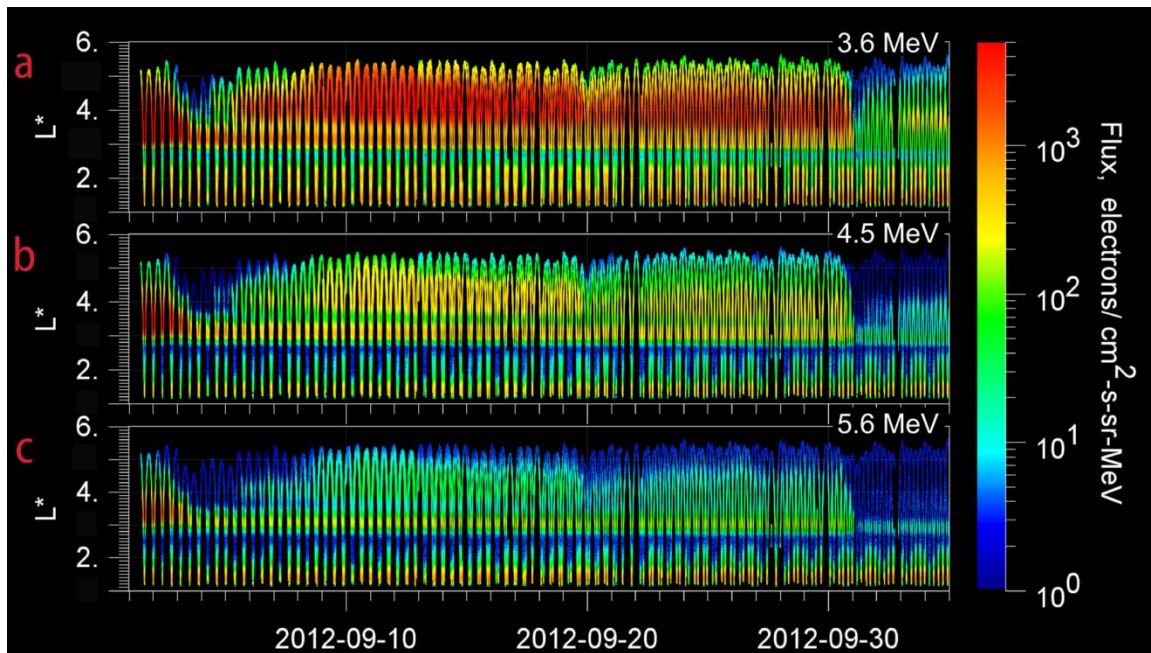


Fig. 1. Energetic electron data from the Radiation Belt Storm Probes (RBSP) satellites in eccentric orbits around the Earth showing several discrete energy channels of the Relativistic Electron-Proton Telescope (REPT) instruments on board the spatially separated RBSP-A and RBSP-B spacecraft. Each panel's vertical axis is the L^* parameter which is effectively the distance in Earth radii at which a magnetic field line crosses the magnetic equatorial plane. The horizontal axis is time from 1 September 2012 to 4 October 2012. Electron differential flux values (in units of electrons/cm²-s-sr-MeV) are in a color-coded logarithmic scale as shown to the right of the figure. (A) Electrons in the energy range $3.2 \leq E \leq 4.0$ MeV. (B) Electrons with $4.0 \leq E \leq 5.0$ MeV. (C) Electrons with $5.0 \leq E \leq 6.2$ MeV.

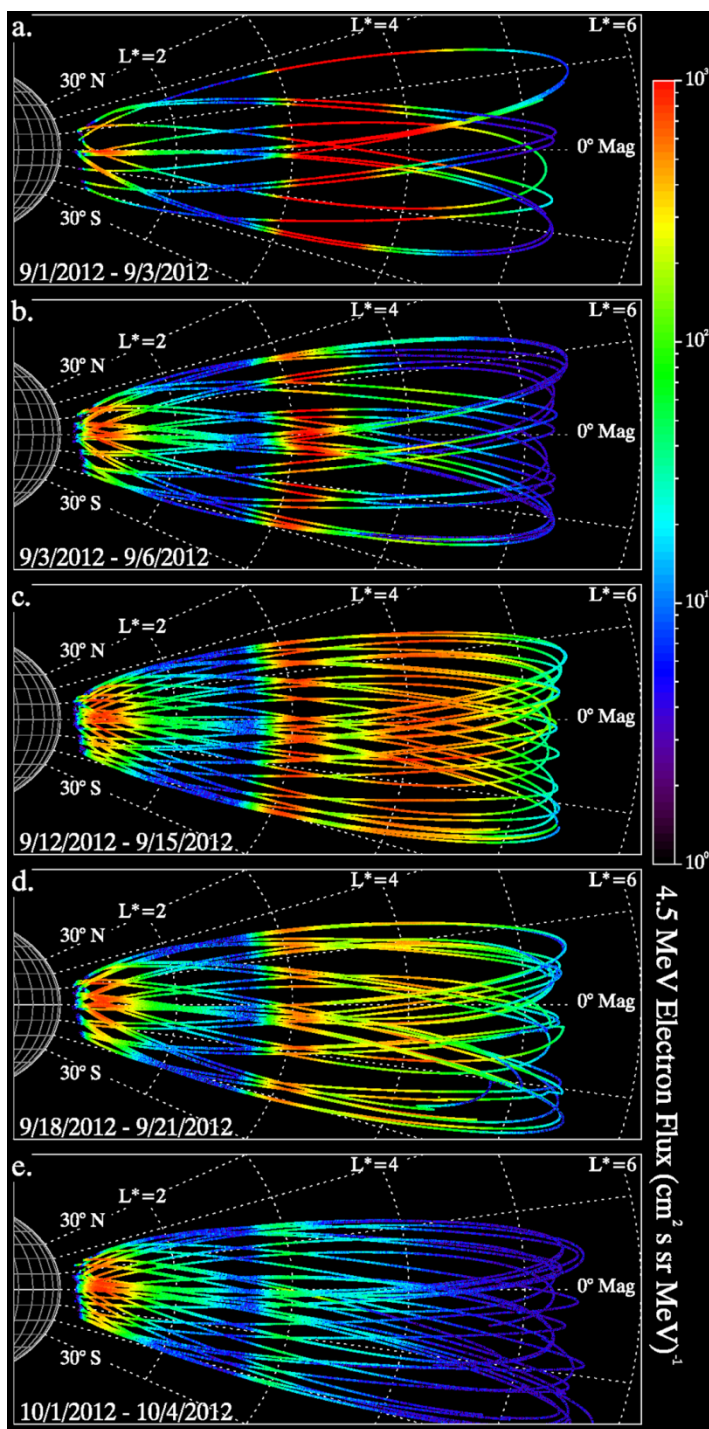


Fig. 2. Meridional plane projections of the REPT-A and REPT-B electron flux (4.0-5.0 MeV) values as shown according to the logarithmic color scale to the right of the figure. Each panel shows a limited interval of time in a magnetic latitude – L^* coordinate system. (A) For 1-3 September the expected two-belt Van Allen zone structure with an inner zone electron population ($L^* < \sim 2.5$), a relatively empty “slot” region ($2.5 < L^* < 3.0$), and an outer zone population ($L^* > 3.0$). (B) From 3 September through 6 September only an intense belt of electrons remains in the range $3.0 < L^* < 3.5$; the inner zone and traditional slot region have not changed. (C) The “storage ring” belt, or torus, feature persists at $3.0 < L^* < 3.5$ while a new slot region is seen at $3.5 < L^* < 3.8$ and a completely new outer zone population has formed at $L^* > 3.8$. (D) The storage ring feature remains while the outer zone at $L^* > 3.8$ decays away. (E) The entire outer zone ($L^* > \sim 3.0$) has virtually disappeared at these energies.

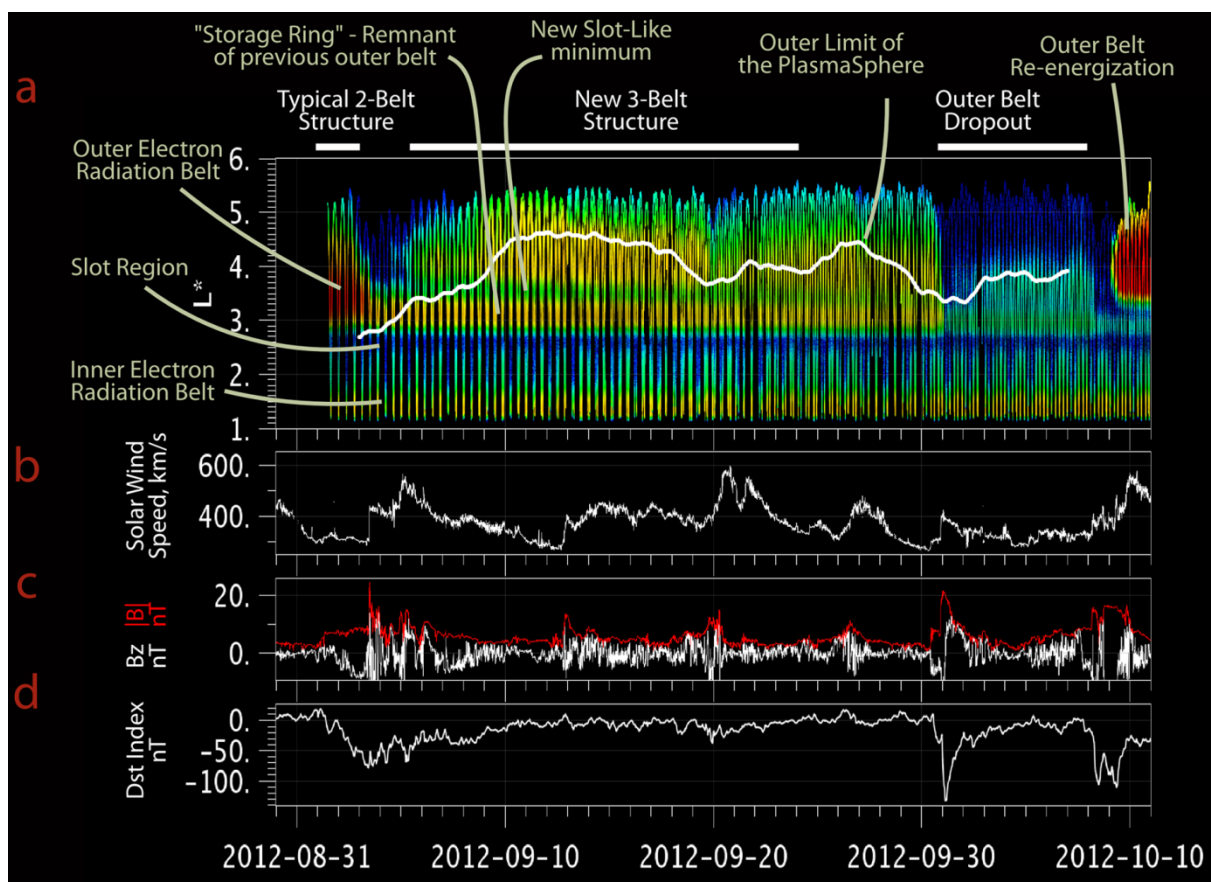


Fig. 3. (A) Similar to panel (B) of Fig. 1 but including the plasmapause, the outer boundary of the plasmasphere (26) for the period 1 September to 7 October 2012. The white curve over-plotted upon the color-coded electron particle flux data in Fig. 3A shows the modeled, 3-day averaged plasmapause radial location that is in agreement with concurrent plasma wave data (17, 27, 28). **(B)** The concurrently measured solar wind speed upstream of the Earth's magnetosphere. **(C)** The interplanetary magnetic field for the interval under study. **(D)** The geomagnetic activity index Dst for the period under study.

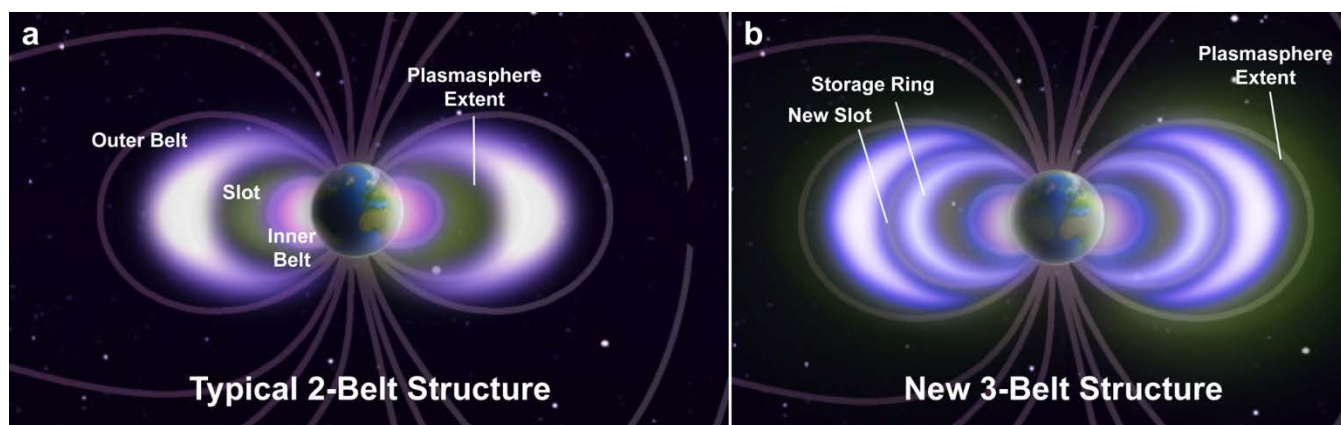


Fig. 4. Diagrams providing a cross-sectional view of the Earth's radiation belt structure and relationship to the plasmasphere. (A) A schematic diagram showing the Earth, the outer and inner radiation belts and the normal plasmaspheric location. (B) Similar to (A) but showing a more highly distended plasmasphere and quite unexpected triple radiation belt properties during the September 2012 period. These diagrams show the highest electron fluxes as white and the lowest fluxes as blue. The radiation belts are really 'doughnut' or torus-shaped entities in three dimensions. The Earth is portrayed at the center. Also shown, as a translucent green overlay in each diagram, is the plasmasphere.